Particle-In-Cell/Monte Carlo Simulation of Ion Back Bombardment in Photoinjectors

Ji Qiang, John N. Corlett, and John Staples

Lawrence Berkeley National Laboratory, 1 Cyclotron Road, Berkeley, CA 94720

Abstract. In this paper, we report on studies of ion back bombardment in high average current dc and rf photoinjectors using a particle-in-cell/Monte Carlo method. Using H_2 ion as an example, we observed that the ion density and energy deposition on the photocathode in rf guns are order of magnitude lower than that in a dc gun. A higher rf frequency helps mitigate the ion back bombardment of the cathode in rf guns.

Keywords: particle-in-cell/Monte Carlo, ion back bombardment.
PACS: 29.25.Bx,29.27.Bd;

INTRODUCTION

The ion back bombardment could cause significant decrease of quantum efficiency of the cathode in photoinjectors by either surface pollution or cathode material destruction. It is a major factor that limits the photocathode lifetime in some high average current photoinjectors [1-2]. In previous studies, single particle tracking and simplified analytical model were used to estimate the ion generation and impact deposition on the cathode of the gun [3-4]. In this paper, we used a self-consistent particle-in-cell/Monte Carlo method to simulate ion generation and ion back bombardment in both dc and rf photoinjectors.

COMPUTATIONAL MODEL

We have used the IMPACT-T code in this study. The IMPACT-T code is a three-dimensional quasi-static particle-in-cell (PIC) code to simulate charged particle transport in dc or rf photoinjectors [5]. Here, a bunch of photo-electrons emitted from the cathode will be transported through the injector subject to both the external accelerating/focusing forces and self-consistent space-charge forces. The electron beam collides with the background gas and produces ions through the electron-impact ionization. The production of ions is simulated using a Monte Carlo method given the ionization probability. Here, the probability of production of an ion by an electron impact ionization at each time step is given by [6]:

$$p_i = 1 - \exp(-n_{gas}\sigma v dt)$$

Where n_{gas} is the density of background gas species, σ is the electron impact ionization cross section, v is the relative speed between the electron and the gas molecule, and dt is the time step size. Given the ionization probability for an electron,

a uniformly distributed random number ξ is generated. If $\xi < p_i$, the ionization occurs, an ion particle is generated. Once an ion is generated, it will be subject to both the external forces of accelerating/focusing fields and the space-charge forces from the electrons. The space-charge forces among the ions and the space-charge forces on the electrons from the ions are neglected given the fact that the number of ions is much less than the number of electrons. The initial spatial location of the ion is assumed to be the same as that of the electron. The initial velocity of ion is sampled from a Gaussian distribution with given initial gas temperature. Here, we also neglect the detailed momentum exchange between the electron and the ion given the fact that this is small compared with the large external accelerating forces.

SIMULATION RESULTS

Using above computational model, we studied ion back bombardment in a VHF injector proposed at Lawrence Berkeley National Laboratory [7]. Figure 1 shows the kinetic energy and transverse rms size of the electron beam with 0.8 nC charge through the injector. The initial laser pulse is assumed to be a flat-top distribution with 1 mm radius and about 100 ps full length. The kinetic energy of the electron beam out of the injector is about 750 keV. The transverse rms size has blown up significantly due to the strong space-charge effects.

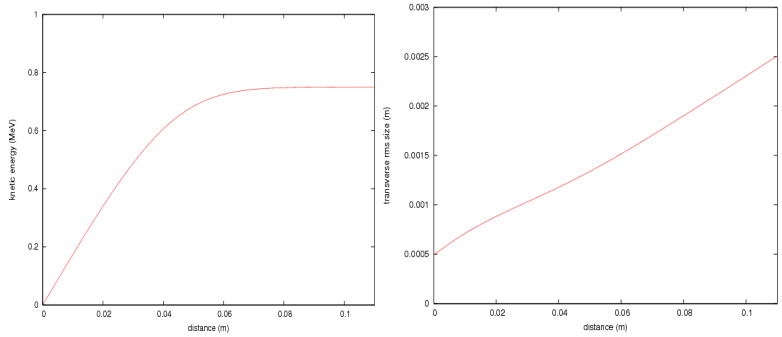

FIGURE 1. Electron kinetic energy (left) and transverse rms size (right) through the injector.

In this study, we used hydrogen molecule as our test case. Figure 2 shows the electron impact ionization cross section of the hydrogen molecule as a function of the electron energy [8]. The ionization cross section peaks around 50 eV electron energy and decreases quickly towards the higher energy.

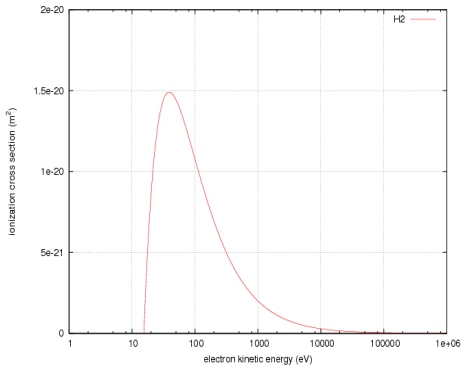

FIGURE 2. Electron impact ionization cross section of H_2 as a function of electron energy.

Using the cross section of hydrogen molecule and the particle-in-cell/Monte Carlo method, we simulated the H_2 ion back bombardment of the cathode for the cavity with 0 MHz rf frequency, i.e. dc gun, 100 MHz rf frequency, and 200 MHz rf frequency. Here, we have assumed that all three cases have the same longitudinal electric field profile. The background gas is assumed to be 10^{-6} Torr in order to improve the statistic of H_2 ions. The following simulation results need to be scaled with corresponding gas pressure for a realistic pressure between 10^{-11} and 10^{-10} Torr in the photoinjectors. The electron beam repetition rate is 1 MHz. Figure 3 shows the H_2 back bombardment ion density distribution on the cathode as a function radial distance for three frequencies. It is seen that for the DC gun, the peak of the H_2 ion density is about one order of magnitude higher than that of the rf guns. It peaks on the axis and decreases toward the edge that is larger than the initial electron beam size. This is due to the fact that all ions generated inside the gun when the electron beam passes through the cavity are accelerated back to the cathode. For the rf gun case, the ion density profile on the cathode is quite flat with a much smaller amplitude compared with the dc gun case. The maximum radial distance of ions that is slightly more than 1 mm for the rf guns is also much smaller than that for the dc gun. This suggests that the major contribution of ions to the back bombardment came from the ions generated not far from the cathode where the electron beam has not blown up significantly. The ions that generated further downstream are not able to reach the cathode before the change of sign of accelerating field in rf guns.

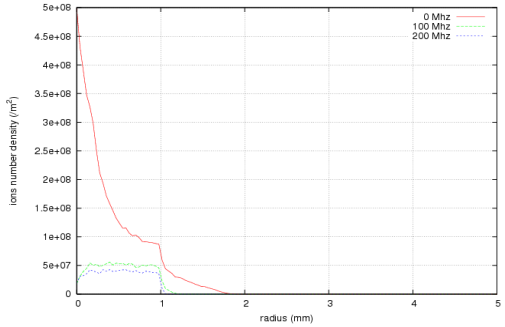

FIGURE 3. H_2 ion particle radial density distribution at cathode with 0 MHz DC gun, 100 MHz, and 200 MHz rf guns.

Figure 4 shows the H_2 ion energy distribution on the cathode for the three different frequencies. It is seen that for the dc gun case, the maximum kinetic energy extends to about 750 keV that corresponds to the potential voltage across the accelerating gap. There are two peaks in the ion particle distribution, one is near the low energy, and the other is near the high energy. The peak near the low energy is due to the contribution from the peak of cross section near the low energy as shown in Figure 2. The peak near the high energy is due to the fact that the ionization probability depends also on the relative velocity between the electrons and background gas. This compensates the decreasing of ionization cross section for high energy electrons. All ions generated from 5 cm to 11 cm by high energy electron near the tail of accelerating field are accelerated back to the cathode acquiring a large energy. For the rf guns, the situation is quite different. The ions generated by high energy electron downstream may not be able to move back to the cathode. The main contribution to the cathode is the ions generated not far from the cathode. The ions oscillate inside the time-dependent field also acquiring a small energy when they reach the cathode. This accounts for the single peak of ion energy distribution dominated by the ionization cross section and much smaller maximum ion energy amplitude than that in the dc gun case. This maximum ion energy amplitude also decreases from the 100 MHz rf gun to the 200 MHz rf gun.

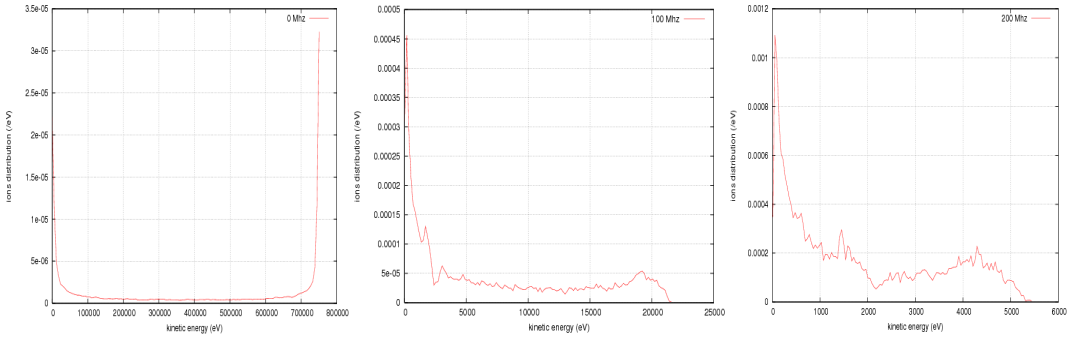

FIGURE 4. H_2 ion normalized energy distribution at cathode with 0 MHz DC gun (left), 100 MHz (middle), and 200 MHz (right) rf guns.

Figure 5 shows the power deposition on the cathode as a function of radial distance for the three frequency cases. Given the fact that H_2 ions have a lower density and a lower energy in the rf guns than those in the dc gun, this results in three order of magnitude less power deposition on the cathode compared with the dc gun case as shown in the figure.

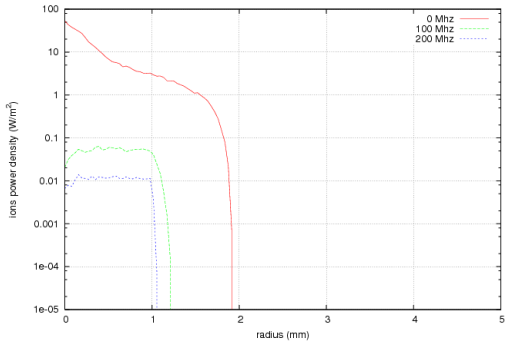

FIGURE 5. H_2 ion power radial density distribution at cathode with 0 MHz DC gun, 100 MHz, and 200 MHz rf guns.

DISCUSSIONS AND CONCLUSIONS

In above sections, we have presented numerical simulations of H_2 ion back bombardment in both dc and rf photoinjectors using a particle-in-cell Monte Carlo method. These results suggest that using an rf photo gun could significantly lower the ion density and energy deposition on the cathode. This will help improve the lifetime of the photocathode in an rf gun. Meanwhile, we also observed some ions trapped inside the rf gun due to the time dependent electromagnetic cavity fields and space-charge fields of electron beam. Further studies are needed to assess the potential effects of those trapped ions.

ACKNOWLEDGMENTS

We would like to thank Drs. S. Lidia and F. Sannibale for helpful discussions. This research was supported by the Office of Science of the U.S. Department of Energy under Contract No. DE-AC02-05CH11231. This research used resources of the National Energy Research Scientific Computing Center.

REFERENCES

1. K. Aulenbacher et al., Nucl. Instrum. Methods Phys. Res., A 319, 498 (1997).
2. C. K. Sinclair et al., Phys. Rev. ST Accel. Beams 10, 023501 (2007).
3. J. W. Lewellen, Phys. Rev. ST Accel. Beams 5, 020101 (2002).
4. E. Pozdeyev, Phys. Rev. ST Accel. Beams 10, 083501 (2007).
5. J. Qiang, S. Lidia, R. D. Ryne, C. Limborg, Phys. Rev. ST Accel. Beams 9, 044204 (2006).
6. J. Wang, P. Liewer, and E. Huang, J. Supercomputing, 10, 331 (1997).
7. K. Baptiste, J. Corlett, S. Kwiatkowski, S. Lidia, J. Qiang, F. Sannibale, K. Sonnad, J. Staples, S. Virostek, R. Wells, Nucl. Instrum. Methods Phys. Res., A 599, 9 (2009).
8. M. Reiser, “Theory and Design of Charged Paricle Beams,” Joh Wiley & Sons, Inc., New York, 1994.